Supporting Information

Morpholine-Linked Metal Phthalocyanine Covalent Organic Frameworks for Enhanced Photocatalytic CO_2 Reduction

Fuwen Lin, [abe] Wan Lin, [ace] Jing Lin, [ad] Zhiwei Xiao, [ace] Yangdan Hui, [ae] Junlan Chen, [ace] Yaobing Wang *[acd]

[a] CAS Key Laboratory of Design and Assembly of Functional Nanostructures, and Fujian Provincial Key Laboratory of Nanomaterials, State Key Laboratory of Structural Chemistry, Fujian Institute of Research on the Structure of Matter, Chinese Academy of Sciences, Fuzhou 350002, Fujian, P. R. China.

[b] College of Chemistry and Materials Science, Fujian Normal University, Fuzhou, 350007, China.

[c] University of Chinese Academy of Sciences, Beijing 100049, P. R. China.

[d] Fujian Science and Technology Innovation Laboratory for Optoelectronic Information of China, Fuzhou 350108, Fujian, P. R. China.

[e] Fujian College, University of Chinese Academy of Sciences, Fuzhou 350002, P. R. China.

[*] Corresponding Author: wangyb@fjirsm.ac.cn.

Materials and Methods

Chemicals： All the starting materials were purchased from Bide or Admas and used without further purification. Cobalt (II) 1,2,3,4,8,9,10,11,15,16,17,18,22,23,24,25-hexadecafluoro-29H,31H-phthalocyanine ($CoPcF_{16}$), 2,5-Diaminobenzene-1,4-diol (DHA) and 4,4'-Diamino-[1,1'-biphenyl]-3,3'-diol (DHB) were purchased from Bide. Acetonitrile, triethylamine and 1,4-Dioxane were purchased from Adamas-beta®.

Synthesis of Co-DA-COF: $CoPcF_{16}$ (0.03 mmol) and DHA (0.06 mmol) were added to a 10 mL Pyrex vial, and then introduced 1.5 mL 1,4-dioxane. After ultrasonic treatment for 5 minutes, 300 μL of triethylamine was quickly added. The vial was subjected to three cycles of frozen-pump-thawed. And then sealed, 3 days 120 ℃ heating. Upon completion, washed thoroughly by THF and acetone, and dried overnight at 60 ℃, yielding approximately 20 mg of activated sample.

Synthesis of Co-DB-COF: The synthesis followed the same protocol used for Co-DA-COF, substituting DHB for DHA.

Characterization: The products were characterized using powder X-ray diffraction (PXRD) on a RIGAKU SmartLab (2θ range: 2.5-40°, scan rate: 5°/min). Fourier transform infrared (FT-IR) spectra were recorded on a VERTEX70 infrared spectrometer. Solid-state ^{13}C NMR was performed on an AVANCE III spectrometer. Scanning electron microscopy (SEM) was conducted using a Zeiss Sigma 300 at 10 kV. Field-emission transmission electron microscopy (FETEM) images were acquired with a Talos-F200X. X-ray photoelectron spectroscopy (XPS) spectra were collected using an ESCALAB 250xi (Thermo Scientific) with Al Kα radiation. N_2 adsorption-desorption was measured with an ASAP 2020M microporous analyzer (Micromeritics). Solid-state UV-vis diffuse reflectance spectra were obtained using a Lambda 950 spectrophotometer with $BaSO_4$ as the reference.

Photocurrent, Mott-Schottky (MS), and Electrochemical Impedance Spectroscopy (EIS) measurements: A total of 4 mg of catalyst was dispersed in 0.5 mL ethanol and 50 μL of 5 wt% Nafion solution, followed by sonication to prepare a uniform catalyst ink. This ink was then applied to a polished FTO glass substrate and left to air dry. Electrochemical measurements were performed using a CHI 660E workstation in a three-electrode system under illumination from a 300 W Xe lamp (PLSSXE300, Perfect Light, China) with a 420 nm cutoff filter. The catalyst-coated FTO glass served as the photoelectrode, with Pt foil as the counter electrode and Ag/AgCl as the reference electrode. The three electrodes were immersed in a quartz cell containing 0.2 M Na_2SO_4 electrolyte.

CO_2 Photocatalytic Reduction: In a 200 mL photoreactor, 2 mg COF and 10 mg $[Ru(bpy)_3]Cl_2·6H_2O$ were mixed in a solution of MeCN, water, and TEOA (20 mL, 5:3:2 by volume), followed by 30 minutes of sonication. CO_2 was introduced for 30 minutes to purge air from the reactor. CO and H_2 production were monitored using gas chromatography (FULI 9790II). After 2 hours of irradiation, the COF was recovered via centrifugal separation, thoroughly purified with

MeCN and acetone, and subsequently vacuum-dried at 60 ℃. The regenerated solid was reused for five photocatalytic cycles under the same conditions. Potential liquid products were analyzed via ^{1}H NMR spectroscopy (Avance III HD).

In-situ FT-IR spectroscopy measurements: In situ FT-IR experiments were conducted using a Nicolet 6700 FT-IR spectrometer equipped with a liquid nitrogen-cooled MCT detector. During photocatalytic CO_2 reduction, an ATR module with a germanium crystal window was employed. COF powder was placed on the germanium crystal, and a CO_2 photocatalytic reduction system solution was added dropwise. Prior to measurement, the solution was saturated with CO_2. A 300 W Xe lamp (PLSSXE300, Perfect Light, China) with a 420 nm cutoff filter served as the light source for the tests.

Computation details： The first principles calculations were performed by employing the Vienna ab initio simulation package (VASP) with the projected augmented wave (PAW) potentials.[1] The generalized gradient approximation (GGA) Perdew-Burke-Ernzerhof (PBE) exchange-correlation functional was involved in the structural optimization.[2-3] The primitive cells of COFs structure with I4/m spacegroup were energy favorable after the full relaxation. The cutoff energy for the plane-wave basis was set to 500 eV with 5*5*5 in the Brillouin zone for the geometry, and the convergence thresholds of the energy and the force was set to 10^{-4} eV and 0.5 eV/Å, respectively. The orbital calculations were performed by DMol3 with GGA-PBE functional in the fine quality.

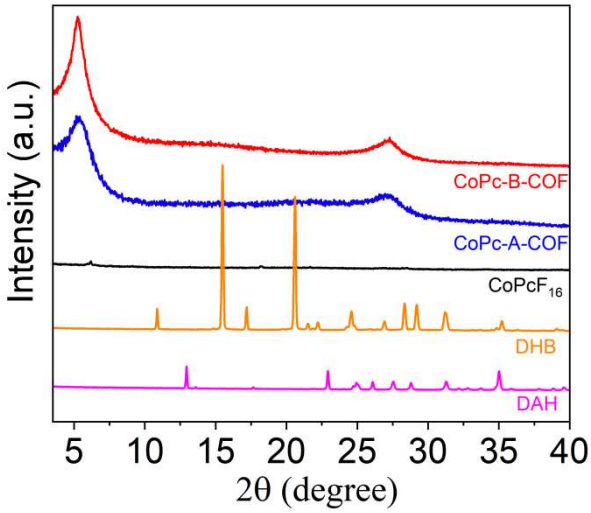

Figure S1. PXRD patterns of Co-DA-COF, Co-DB-COF, DAH, DHB and $CoPcF_{16}$.

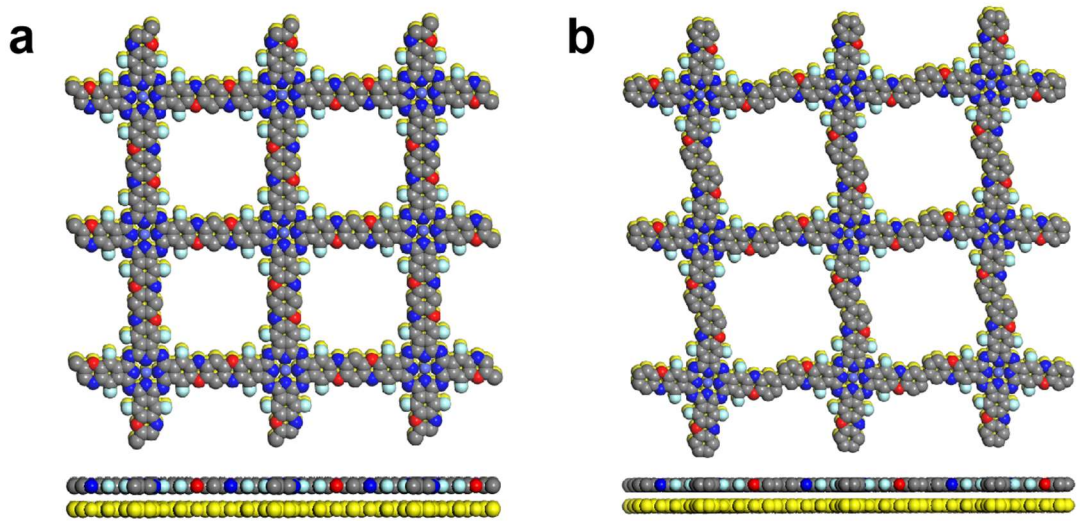

Figure S2. Simulated AA stacking of (a) Co-DA-COF and (b) Co-DB-COF.

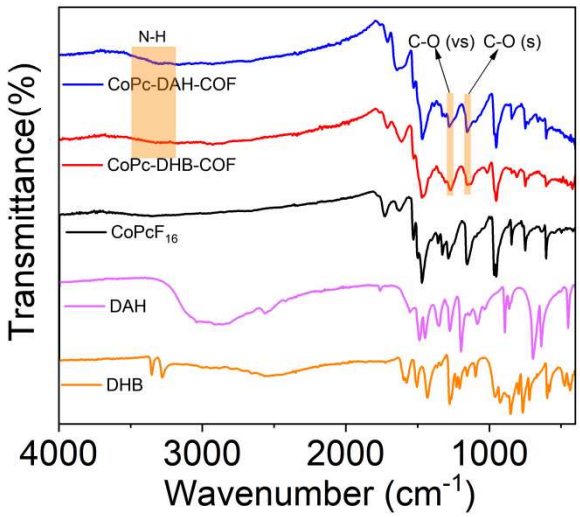

Figure S3. FT-IR spectra of Co-DA-COF, Co-DB-COF, DAH, DHB and $CoPcF_{16}$.

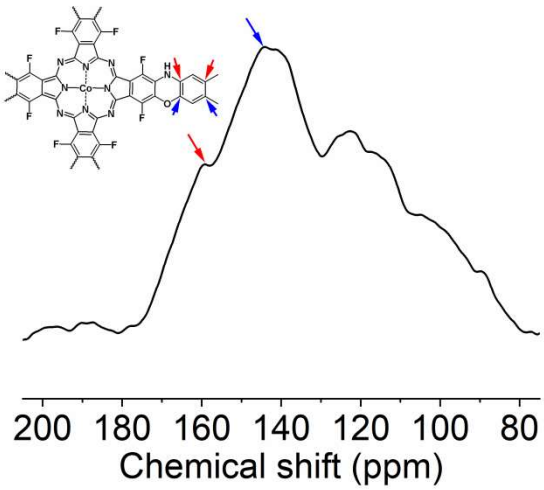

Figure S4. The solid-state ^{13}C CP/MAS NMR spectrum of Co-DA-COF.

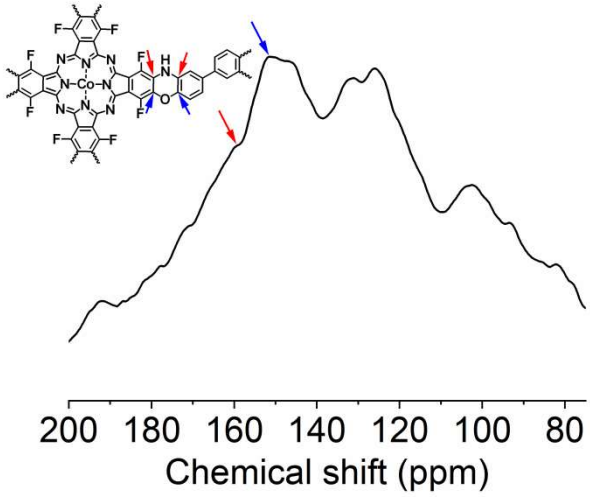

Figure S5. The solid-state ^{13}C CP/MAS NMR spectrum of Co-DB-COF.

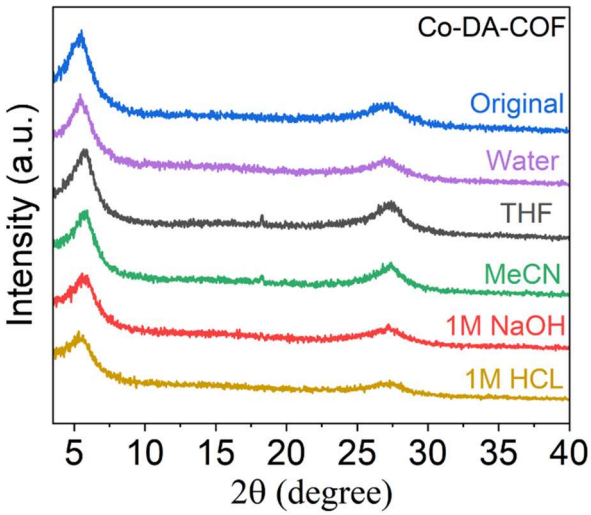

Figure S6. PXRD patterns of Co-DA-COF as-synthesized and after soaked in water, THF, MeCN, HCl(1M) and NaOH(1M) for 7days.

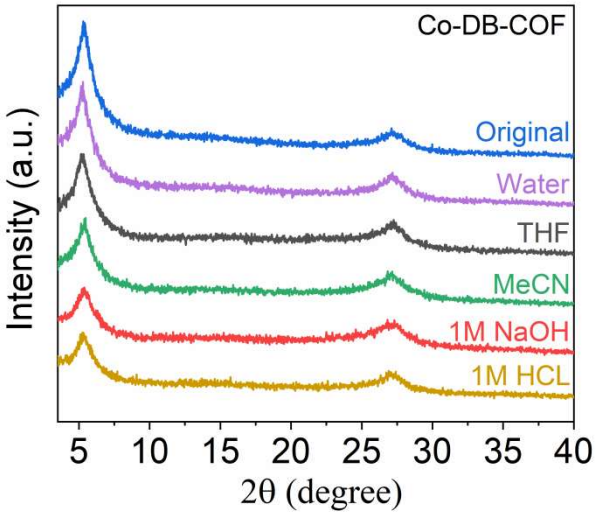

Figure S7. PXRD patterns of Co-DB-COF as-synthesized and after soaked in water, THF, MeCN, HCl(1M) and NaOH(1M) for 7days.

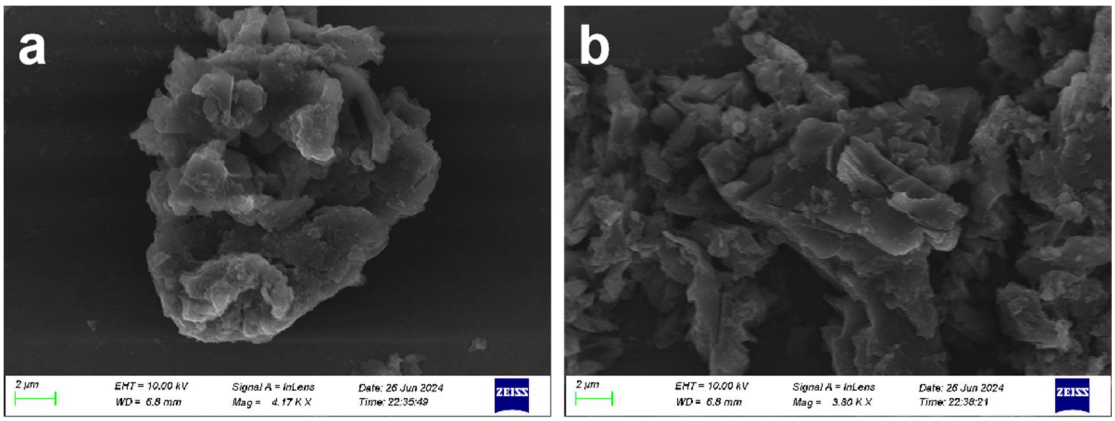

Figure S8. SEM images of (a) Co-DA-COF and (b) Co-DB-COF.

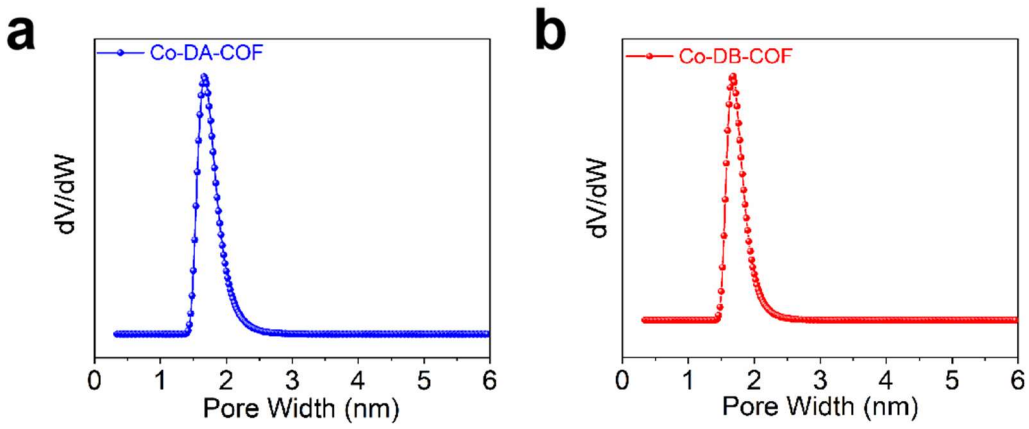

Figure S9. The pore size distribution of (a) Co-DA-COF and (b) Co-DB-COF.

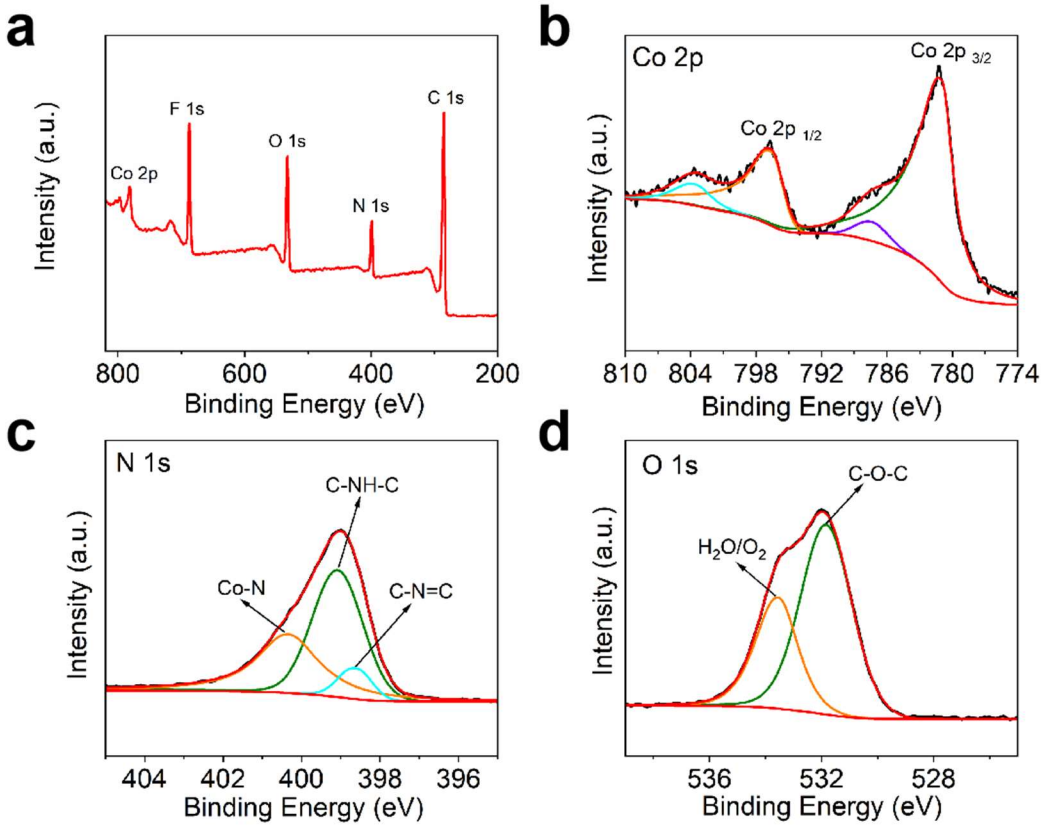

Figure S10. XPS (a) survey, (b) Co 2p, (c) N 1s and (d) O 1s spectra of Co-DA-COF.

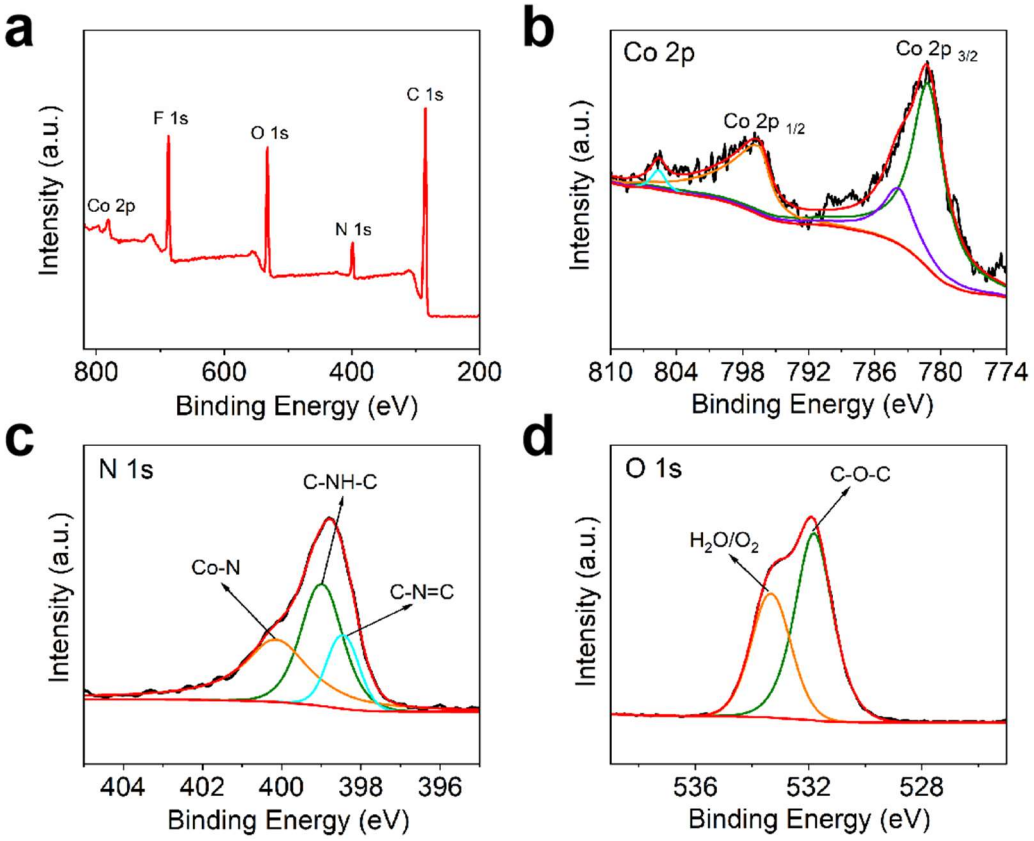

Figure S11. XPS (a) survey, (b) Co 2p, (c) N 1s and (d) O 1s spectra of Co-DB-COF.

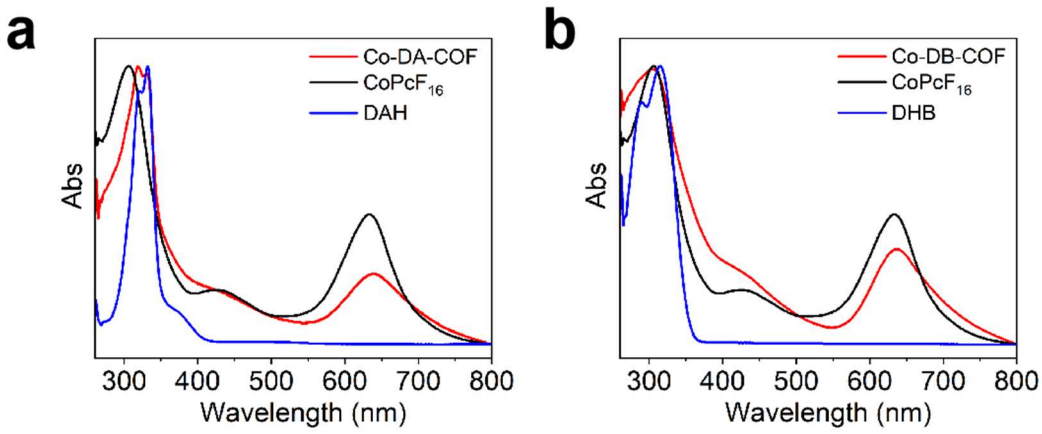

Figure S12. (a) UV-visible pattern of Co-DA-COF, $CoPcF_{16}$ and DAH. (b)UV-visible pattern of Co-DB-COF, $CoPcF_{16}$ and DHB.

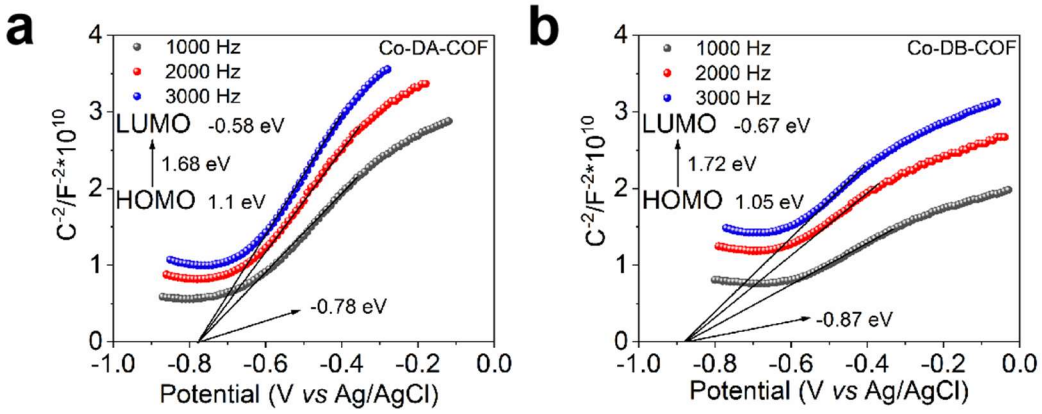

Figure S13. Mott-Schottky curve of (a) Co-DA-COF and (b) Co-DB-COF under neutral conditions.

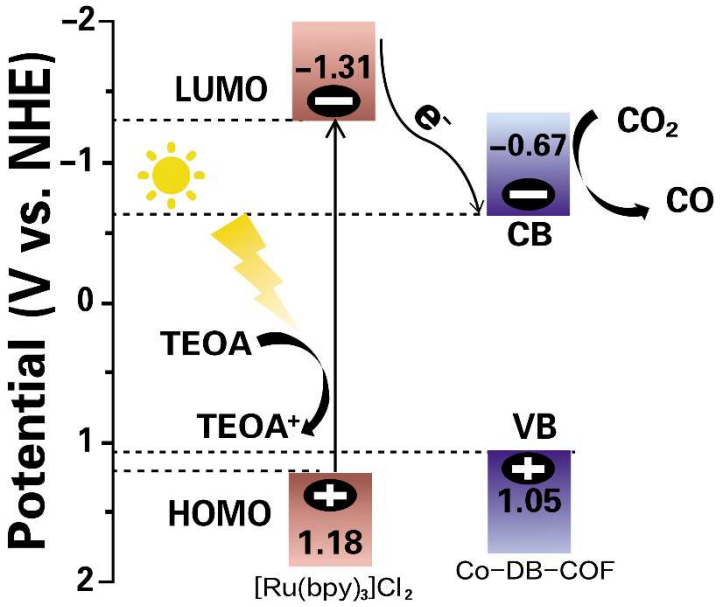

Figure S14. The proposed plausible mechanism for CO_2 photoreduction of Co-DB-COF.

Figure S15. The photo of the photocatalysis equipment.

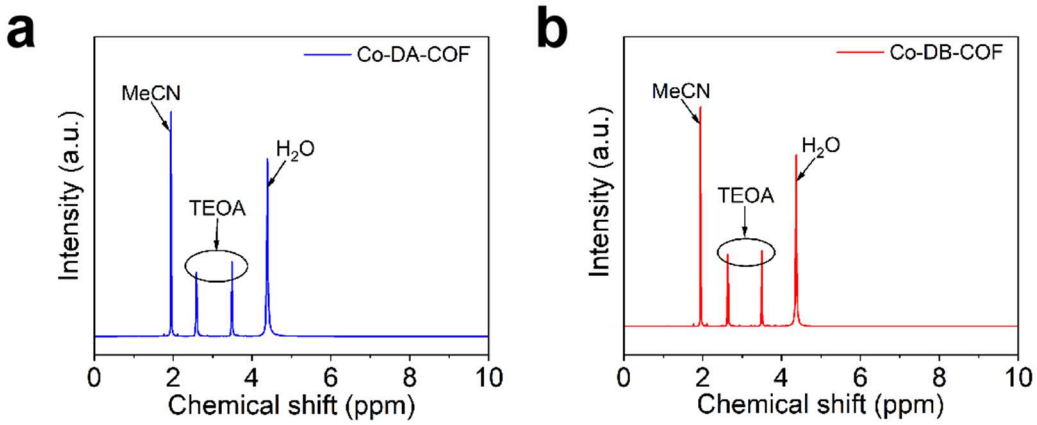

Figure S16. ^{1}H NMR spectra of the liquid products after CO_2 reduction catalyzed by (a) Co-DA-COF and (b) Co-DB-COF. d^6-DMSO was used as the internal standard.

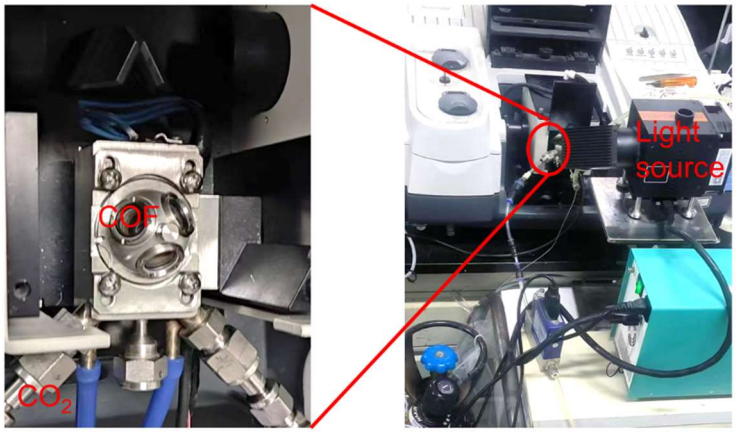

Figure S17. Schematic diagram of in situ FT-IR spectroscopy measurements.

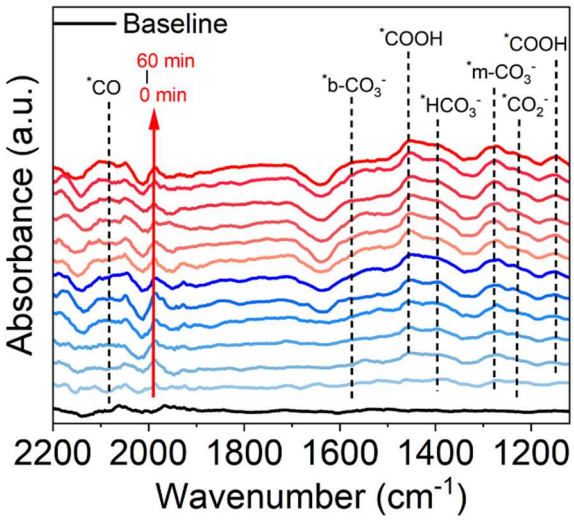

Figure S18. In-situ FTIR spectra of the Co-DA-COF system at room temperature under light.

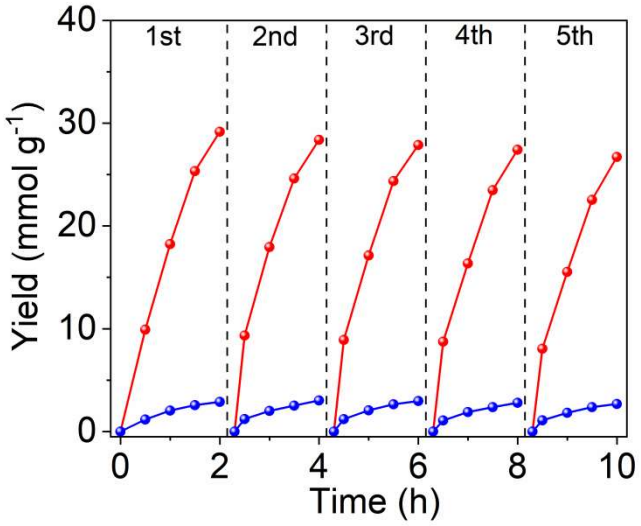

Figure S19. Durability measurements of Co-DA-COF of CO_2 photocatalytic reduction process to CO (red) and H_2 (blue).

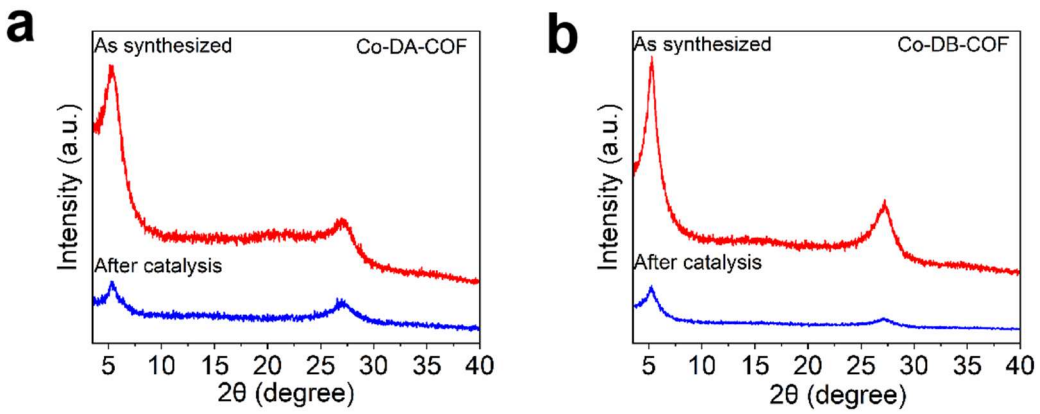

Figure S20. XRD of Co-DA-COF and Co-DB-COF before and after photocatalytic CDRR performance.

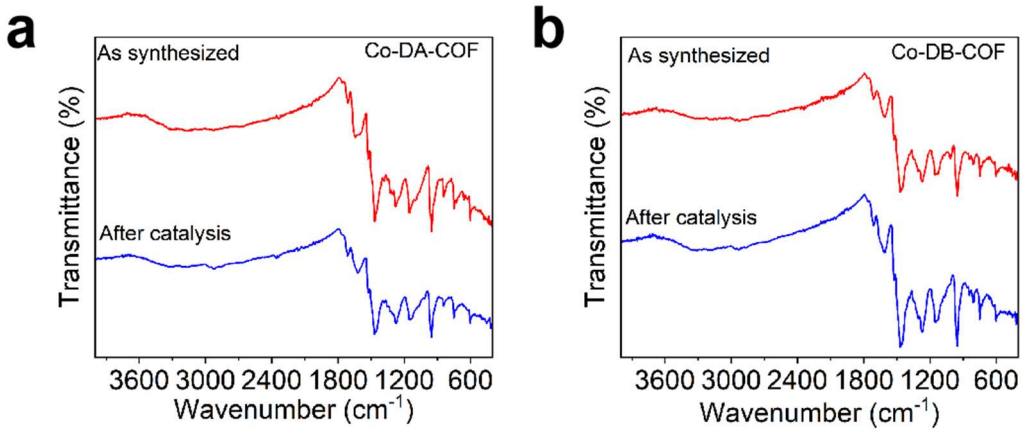

Figure S21. FTIR of Co-DA-COF and Co-DB-COF before and after photocatalytic CDRR performance.

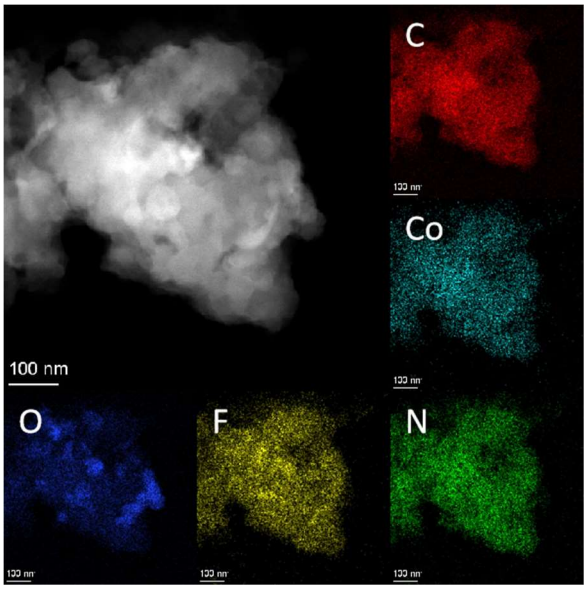

Figure S22. TEM and EDS of Co-DA-COF after photocatalytic CDRR performance.

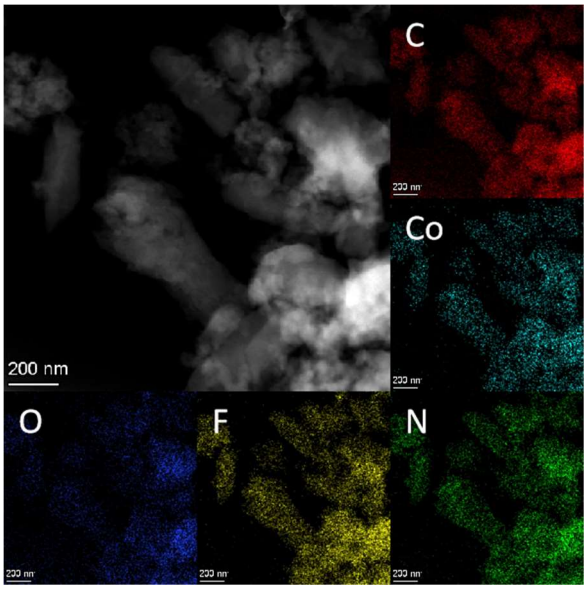

Figure S23. TEM and EDS of Co-DB-COF after photocatalytic CDRR performance.

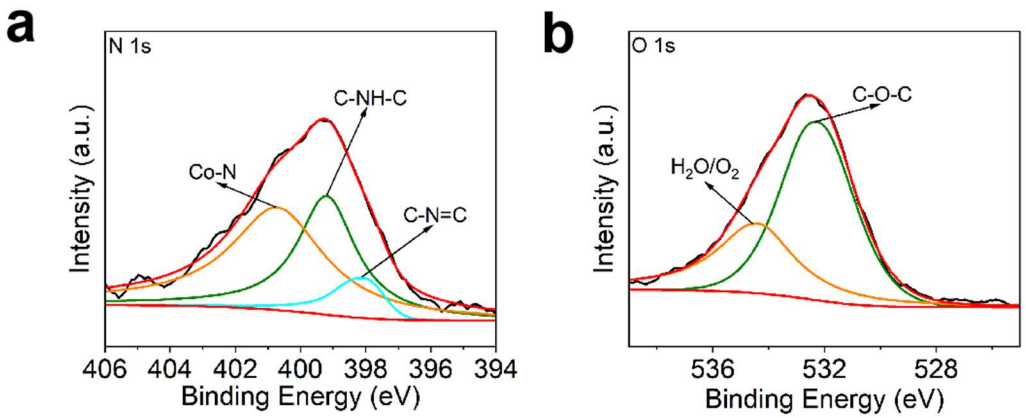

Figure S24. XPS of Co-DA-COF after photocatalytic CDRR performance.

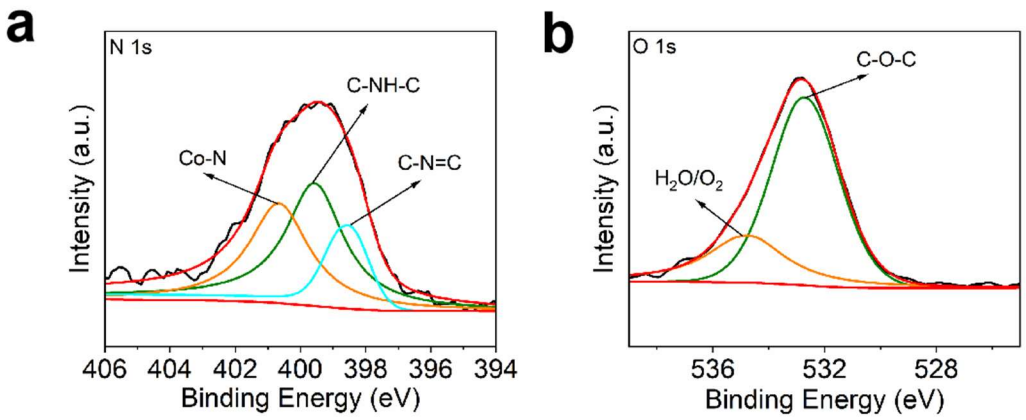

Figure S25. XPS of Co-DB-COF after photocatalytic CDRR performance.

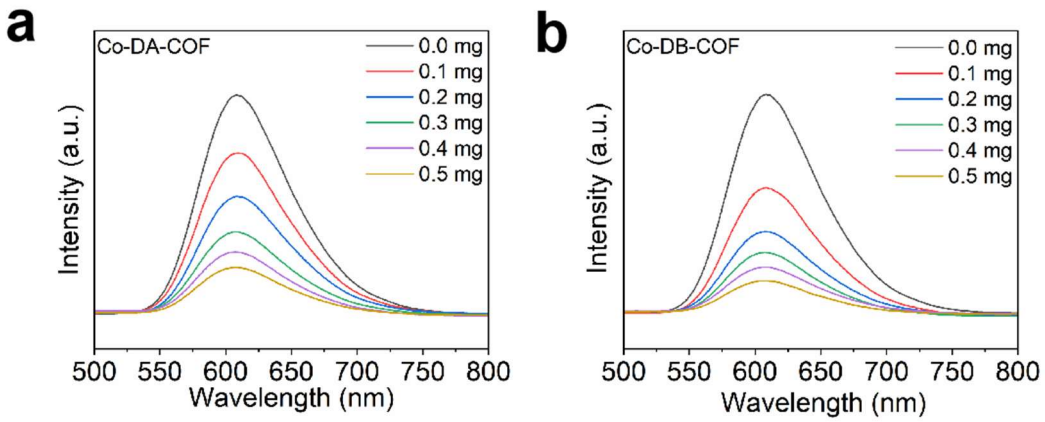

Figure S26. Changes of fluorescence spectra of $[Ru(bpy)_3]Cl_2 \cdot 6H_2O$ upon adding (a) Co-DA-COF and (b) Co-DB-COF (λex = 450 nm).

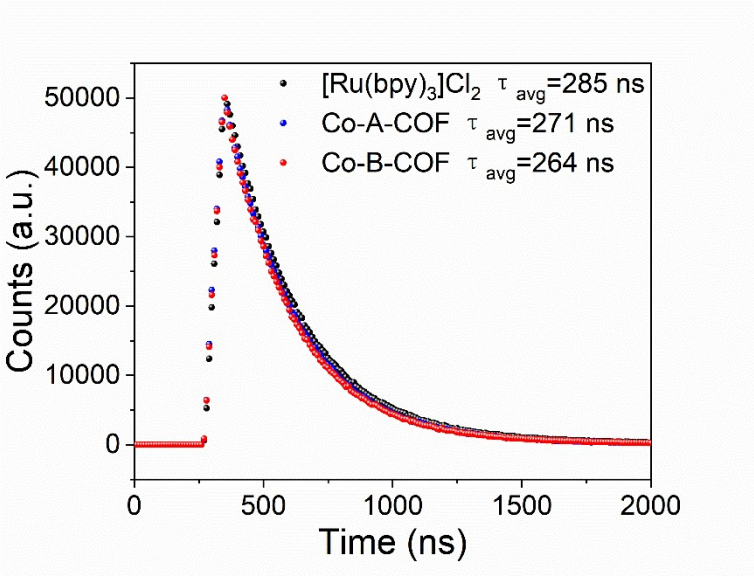

Figure S27. Time-resolved PL decay spectra of $[Ru(bpy)_3]Cl_2 \cdot 6H_2O$ was with Co-DA-COF and Co-DB-COF (λex = 450 nm and λem = 610 nm).

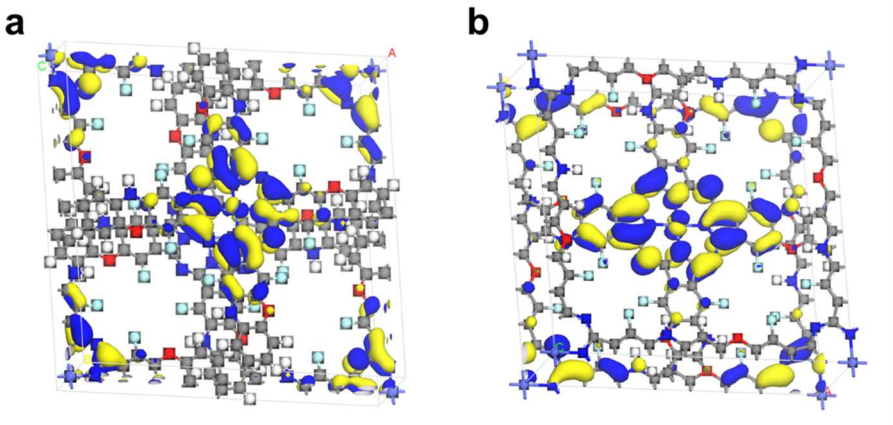

Figure S28. The detail of LUMO of Co-DB-COF and Co-DA-COF.

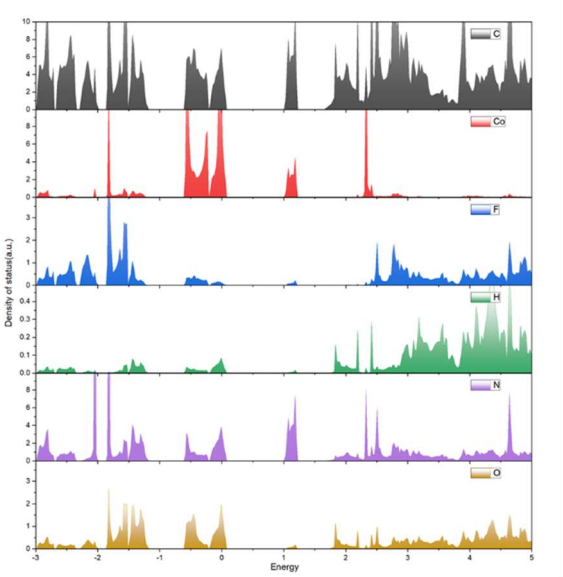

Figure S29. The projected density of status of Co-DB-COF.

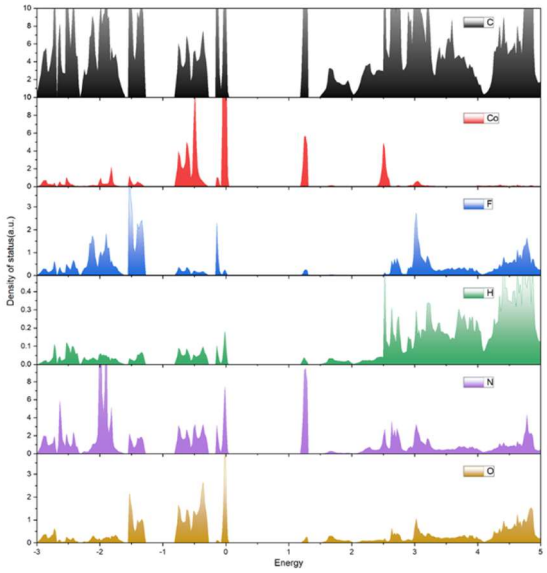

Figure S30. The projected density of status of Co-DA-COF.

Table S1. Performance comparison of COF-based photocatalysts for photocatalytic CO_2 reduction.[4-29]

Photocatalyst	Photosensitizers	Sacrificial Agent	Medium	CO Yield (μmol g-1 h-1)	CO (%)	
Co-DA-COF	**$[Ru(bpy)_3]Cl_2·6H_2O$**	**TEOA**	**MeCN/H_2O (v/v=5/3)**	**20851.6**	**90.5%**	**This work**
Co-DB-COF	**$[Ru(bpy)_3]Cl_2·6H_2O$**	**TEOA**	**MeCN/H_2O (v/v=5/3)**	**25682.2**	**92.3%**	**This work**
Ni-TAPT-COF	$[Ru(bpy)_3]Cl_2·6H_2O$ 2,2′-bipyridine	BIH	MeCN/H_2O (v/v=5/1)	25500	98.8%	4
Co/Cu_3-TPA-COF	$[Ru(bpy)_3]Cl_2·6H_2O$ 4,4′-dimethyl-2,2′-bipyridine	TEOA	MeCN/H_2O (v/v=7/1)	25247.7	80.2%	5
USTB-11(Cu,Ni)	$[Ru(bpy)_3]Cl_2·6H_2O$ 2,2′-bipyridine	TEOA	MeCN/H_2O (v/v=3/1)	22130	98%	6
Co-2,3-DHTA-COF	$[Ru(bpy)_3]Cl_2·6H_2O$	TEOA	MeCN/H_2O (v/v=4/1)	18000 ± 700	95.7%	7
EPCo-COF-AT	$[Ru(bpy)_3]Cl_2·6H_2O$	TEOA	MeCN/H_2O (v/v=1/1)	17695.1	97.8%	8
JUC-640-Co	$[Ru(bpy)_3]Cl_2·6H_2O$	BIH	MeCN/H_2O (v/v=2/3)	15138.9	94.4%	9
EPCo-COF	$[Ru(bpy)_3]Cl_2·6H_2O$	TEOA	MeCN/H_2O (v/v=1/1)	14133.8	85.1%	8
CoPor-DPP-COF	$[Ru(bpy)_3]Cl_2·6H_2O$	TIPA	MeCN/H_2O (v/v=5/3)	10200	82%	10
COF-367-CoNSs	$[Ru(bpy)_3]Cl_2·6H_2O$	Ascorbic Acid	0.1 M $KHCO_3$	10162	78%	11
Co-PyPor-COF	$[Ru(bpy)_3]Cl_2·6H_2O$	TEOA	MeCN/H_2O (v/v=10/3)	9645	96.7%	12
Co-THD-COF	$[Ru(bpy)_3]Cl_2·6H_2O$ 2,2′-bipyridine	TEOA BIH	MeCN/H_2O (v/v=3/1)	9357	95.1%	13
Ni-COF	$[Ru(bpy)_3]Cl_2·6H_2O$	TEOA	MeCN/H_2O (v/v=3/2)	5310	94.8%	14
Ni-TP-CON	$[Ru(bpy)_3]Cl_2·6H_2O$	TEOA	MeCN/H_2O (v/v=3/1)	4360	95%	15
NiPc-CoPOP	$[Ru(bpy)_3]Cl_2·6H_2O$	TEOA	MeCN/H_2O (v/v=16/1)	4270	54%	16
Ni@TPHH-COF	$[Ru(bpy)_3]Cl_2·6H_2O$	TEOA	MeCN/H_2O (v/v=4/1)	3280	95%	17
HOF-25-Re	$[Ru(bpy)_3]Cl_2·6H_2O$	TIPA	MeCN	3030	92%	18
CoP-TPE-COF	$[Ru(bpy)_3]Cl_2·6H_2O$	TEOA	MeCN/H_2O (v/v=3/2)	2414	61%	19
Co-COF	$[Ru(bpy)_3]Cl_2·6H_2O$	TEOA	MeCN/H_2O (v/v=3/2)	2375	58%	14
H-COF-Ni	$[Ru(bpy)_3]Cl_2·6H_2O$ 2,2′-bipyridine	TEOA	MeCN/H_2O (v/v=3/1)	2312	96%	20
NiPc-NiPOP	$[Ru(bpy)_3]Cl_2·6H_2O$	TEOA	MeCN/H_2O (v/v=9/1)	1940	96%	16
TFBD-COF-Co-SA	$[Ru(bpy)_3]Cl_2·6H_2O$	TEOA	MeCN	1480	90%	21
Co@COF-TVBT-Bpy	$[Ru(bpy)_3]Cl_2·6H_2O$	TEOA	MeCN/H_2O (v/v=4/1)	1132.7	50%	22
CH_3-TPPD	$[Ru(bpy)_3]Cl_2·6H_2O$	TEOA	MeCN/H_2O (v/v=4/1)	1033	79.50%	23
DQTP COF-Co	$[Ru(bpy)_3]Cl_2·6H_2O$	TEOA	MeCN	1020	90%	24
CTF-Bpy-Co	$[Ru(bpy)_3]Cl_2·6H_2O$	TEOA	MeCN/H_2O (v/v=4/1)	1019	83.80%	25
Fe-SAS/TrCOF	$[Ru(bpy)_3]Cl_2·6H_2O$	TEOA	MeCN/H_2O (v/v=3/1)	980.3	96.4%	26
Ni-TpBpy	$[Ru(bpy)_3]Cl_2·6H_2O$ 2,2′-bipyridine	TEOA	MeCN/H_2O (v/v=3/1)	811	96%	27
NiP-TPE-COF	$[Ru(bpy)_3]Cl_2·6H_2O$	TEOA	MeCN/H_2O (v/v=3/2)	525	93%	19
Ni-PCD @ TD-COF	$[Ru(bpy)_3]Cl_2·6H_2O$	TEOA	MeCN/H_2O (v/v=3/1)	480	98%	28
α-Fe_2O_3 @Por-CTF	$[Ru(bpy)_3]Cl_2·6H_2O$	TEOA	DMF	400	93%	29

Reference

1. G. Kresse, J. Furthmüller, *Phys. Rev. B: Condens. Matter Mater. Phys.,* 1996, **54**, 11169.
2. P. E. Blöchl, *Phys. Rev. B: Condens. Matter Mater. Phys.,* 1994, **50**, 17953−17979.
3. J. P. Perdew, K. Burke, M. Ernzerhof, *Phys. Rev. Lett.,* 1996, **77**, 3865.
4. Y. Zhang, Y. Liu, H. Li, G. Bai and X. Lan, *Chem. Eng. J.,* 2024, **489**. 151479.
5. X. Lan, H. Li, Y. Liu, Y. Zhang, T. Zhang and Y. Chen, *Angew. Chem. Int. Edit.,* 2024, **63**, e202407092.
6. X. Wang, X. Ding, Y. Jin, D. Qi, H. Wang, Y. Han, T. Wang and J. Jiang, *Angew. Chem. Int. Edit.,* 2023, **62**, e202302808.
7. Q. Zhang, S. Gao, Y. Guo, H. Wang, J. Wei, X. Su, H. Zhang, Z. Liu and J. Wang, *Nat. Commun.,* 2023, **14***,* 1147.
8. W. Lin, F. Lin, J. Lin, Z. Xiao, D. Yuan and Y. Wang, *J. Am. Chem. Soc.,* 2024, **146**, 16229-16236.
9. J. Ding, X. Guan, J. Lv, X. Chen, Y. Zhang, H. Li, D. Zhang, S. Qiu, H.-L. Jiang and Q. Fang, *J. Am. Chem. Soc.,* 2023, **145***,* 3248-3254.
10. X. Wang, X. Ding, T. Wang, K. Wang, Y. Jin, Y. Han, P. Zhang, N. Li, H. Wang and J. Jiang, *ACS Appl. Mater. Interfaces,* 2022, **14***,* 41122-41130.
11. W. Liu, X. Li, C. Wang, H. Pan, W. Liu, K. Wang, Q. Zeng, R. Wang and J. Jiang, *J. Am. Chem. Soc.,* 2019, **141***,* 17431-17440.
12. T. X. Luan, J. R. Wang, K. Li, H. Li, F. Nan, W. W. Yu and P. Z. Li, *Small*, 2023, **10***,* 2303324.
13. Z.-X. Pan, S. Yang, X. Chen, J.-X. Luo, R.-Z. Zhang, P. Yang, Q. Xu and J.-Y. Yue, *Chem. Eng. J.,* 2024, **493**, 152798.
14. B. Han, X. Ou, Z. Zhong, S. Liang, H. Deng and Z. Lin, *Small,* 2020**, 16***,* 2002985.
15. H. Lv, P. Li, X. Li, A. Chen, R. Sa, H. Zhu and R. Wang, *Chem. Eng. J.,* 2023, **451***,* 138745.
16. X. Y. Dong, Y. N. Si, Q. Y. Wang, S. Wang and S. Q. Zang, *Adv. Mater*., 2021, **33**, 2101568.
17. M. Dong, J. Zhou, J. Zhong, H. T. Li, C. Y. Sun, Y. D. Han, J. N. Kou, Z. H. Kang, X. L. Wang and Z. M. Su, *Adv. Funct. Mater*., 2022, **32***,* 2110136.
18. B. Yu, L. Li, S. Liu, H. Wang, H. Liu, C. Lin, C. Liu, H. Wu, W. Zhou, X. Li, T. Wang, B. Chen and J. Jiang, *Angew. Chem. Int. Edit.,* 2021, **60***,* 8983-8989.
19. H. Lv, R. Sa, P. Li, D. Yuan, X. Wang and R. Wang, *Sci. China Chem*., 2020, **63***,* 1289-1294.
20. S. Yang, R. Sa, H. Zhong, H. Lv, D. Yuan and R. Wang, *Adv. Funct. Mater*., 2022, **32**, 2110694.
21. Y. Yang, Y. Lu, H.-Y. Zhang, Y. Wang, H.-L. Tang, X.-J. Sun, G. Zhang and F.-M. Zhang, *ACS Sustain. Chem. Eng*., 2021, **9***,* 13376-13384.
22. J.-X. Cui, Y.-M. Fu, B. Meng, J. Zhou, Z.-Y. Zhou, S.-M. Liu and Z.-M. Su, *J. Mater. Chem. A.,* 2022, **10**, 13418-13427.
23. M. Dong, W. Li, J. Zhou, S. Q. You, C. Y. Sun, X. H. Yao, C. Qin, X. L. Wang and Z. M. Su, *Chin. J. Chem*., 2022, **40***,* 2678-2684.
24. M. Lu, Q. Li, J. Liu, F.-M. Zhang, L. Zhang, J.-L. Wang, Z.-H. Kang and Y.-Q. Lan, *Appl. Catal. B-Environ*., 2019, **254***,* 624-633.
25. X. Hu, L. Zheng, S. Wang, X. Wang and B. Tan, *Chem. Commun*., 2022, **58***,* 8121-8124.
26. L. Ran, Z. Li, B. Ran, J. Cao, Y. Zhao, T. Shao, Y. Song, M. K. H. Leung, L. Sun and J. Hou, *J. Am. Chem Soc.,* 2022, **144***,* 17097-17109.
27. W. Zhong, R. Sa, L. Li, Y. He, L. Li, J. Bi, Z. Zhuang, Y. Yu and Z. Zou, *J. Am. Chem. Soc*., 2019, **141***,* 7615-7621.

28. H. Zhong, R. Sa, H. Lv, S. Yang, D. Yuan, X. Wang and R. Wang, *Adv. Funct. Mater*., 2020, **30***,* 2002654.
29. S. Zhang, S. Wang, L. Guo, H. Chen, B. Tan and S. Jin, *J. Mater. Chem. C.,* 2020, **8***,* 192-200.